

ANL/PHY/CP-94005

Measurements with radioactive beams at ATLAS

K. E. Rehm

Argonne National Laboratory, Physics Division, 9700 South Cass Av., Argonne, IL 60439, USA

RECEIVED
OCT 28 1999

Abstract. Reactions of interest to nuclear astrophysics have been studied with radioactive beams at the ATLAS accelerator. Using a modified ISOL technique, beams of ^{18}F ($T_{1/2}=110\text{min}$) and ^{56}Ni ($T_{1/2}=6.1\text{d}$) were produced and the reactions $^{18}\text{F}(\text{p},\alpha)^{15}\text{O}$, $^{18}\text{F}(\text{p},\gamma)^{19}\text{Ne}$, and $^{56}\text{Ni}(\text{d},\text{p})^{57}\text{Ni}$ have been investigated. The results indicate that the $^{18}\text{F}(\text{p},\gamma)$ route is a small contributor to the breakout from the hot CNO cycle into the rp process, while the $^{56}\text{Ni}(\text{p},\gamma)^{57}\text{Cu}$ rate is about ten times larger than previously assumed.

1. Introduction

The development of radioactive ion beams[1] during the last ten years has opened many new research opportunities in the area of nuclear astrophysics. While in quiescent hydrogen burning the nuclear reactions inside a star involve mainly stable isotopes, the cataclysmic events at the end of a star's life happen on such a rapid time scale that reactions with short-lived isotopes play the dominant role. These conditions occur in various stellar explosions, such as novae, supernovae and X-ray bursts[2]. The network of nuclear reactions that transforms lighter CNO material to heavier elements involves hundreds of reaction rates. These processes have been simulated in network calculations[3] using reaction rates which were obtained from theoretical (Hauser-Feshbach) estimates. If the excitation energy in the compound system is high enough these estimates are usually quite reliable. For reactions involving nuclei in the vicinity of closed shells, however, in the proton capture reactions states at low excitation energies are populated and, thus, properties of the individual levels become important. In this contribution we discuss two examples of reactions in the vicinity of ^{18}F and ^{56}Ni , where nuclear structure effects play a dominant role.

2. Beam production techniques

Since the half-lives of ^{18}F ($T_{1/2}=110\text{ min}$) and ^{56}Ni ($T_{1/2}=6.1\text{d}$) are relatively long, a modified version of the ISOL technique[4] was used for generating the radioactive ion beams. The ^{18}F material was produced by bombarding enriched H_2^{18}O water with a 11

DISCLAIMER

This report was prepared as an account of work sponsored by an agency of the United States Government. Neither the United States Government nor any agency thereof, nor any of their employees, make any warranty, express or implied, or assumes any legal liability or responsibility for the accuracy, completeness, or usefulness of any information, apparatus, product, or process disclosed, or represents that its use would not infringe privately owned rights. Reference herein to any specific commercial product, process, or service by trade name, trademark, manufacturer, or otherwise does not necessarily constitute or imply its endorsement, recommendation, or favoring by the United States Government or any agency thereof. The views and opinions of authors expressed herein do not necessarily state or reflect those of the United States Government or any agency thereof.

DISCLAIMER

**Portions of this document may be illegible
in electronic image products. Images are
produced from the best available original
document.**

MeV proton beam from the medical cyclotron at the University of Wisconsin. After a chemical separation the ^{18}F material was mounted in a copper insert for a negative ion sputter source (SNICS) which is installed at the tandem injector of the superconducting ATLAS accelerator at Argonne National Laboratory. Details of the source preparation technique and the beam intensities obtained in actual experiments are given in Ref.[5].

The ^{56}Ni source material was produced via the $^{58}\text{Ni}(\text{p},\text{p}2\text{n})^{56}\text{Ni}$ reaction by bombarding a small (125 mg) ^{58}Ni pellet with a 50 MeV proton beam from the injector of the Intense Pulsed Neutron Source at Argonne National Laboratory. Taking into account the cross section of the ($\text{p},\text{p}2\text{n}$) reaction, and the size of the beam spot of the proton beam, a fraction of $\sim 5 \times 10^{-6}$ of the ^{58}Ni nuclei was converted into ^{56}Ni . Because of the larger cross section of the $^{58}\text{Ni}(\text{p},2\text{p}n)^{56}\text{Co}$ reaction, the source material contained about 10 times more ^{56}Co , which due to the small mass difference $\Delta m(^{56}\text{Ni} - ^{56}\text{Co})/m = 3.5 \times 10^{-5}$ is difficult to suppress, even using a high resolution mass separator. The ^{56}Ni pellet was also mounted in a copper insert for the negative ion sputter source. Further details can be found in Ref. [6].

3. The Breakout from the hot CNO cycle to the rp-process via the $^{18}\text{F}(\text{p},\gamma)^{19}\text{Ne}$ reaction

The rapid proton (rp) capture process is a series of (p,γ) and (p,α) reactions followed by β^+ decays, where nuclei up to ^{56}Ni and beyond are produced. The border line between the hot CNO cycle and the rp process passes through ^{19}Ne since the reaction Q values in this mass region are such that, once nuclei beyond ^{19}Ne are formed, no recycling into lighter CNO material is possible. The $^{18}\text{F}(\text{p},\gamma)^{19}\text{Ne}$ reaction is, together with the $^{15}\text{O}(\alpha,\gamma)^{19}\text{Ne}$ and the $^{18}\text{Ne}(\alpha,\text{p})^{21}\text{Na}$ reactions, one of the pathways leading from the hot CNO cycle into the rp process. However, due to the positive Q value of the $^{18}\text{F}(\text{p},\alpha)^{15}\text{O}$ reaction, the contribution of the $^{18}\text{F}(\text{p},\gamma)$ route to the breakout from the hot CNO cycle depends strongly on the cross section ratio $\sigma[^{18}\text{F}(\text{p},\gamma)]/\sigma[^{18}\text{F}(\text{p},\alpha)]$.

The cross section of the $^{18}\text{F}(\text{p},\alpha)^{15}\text{O}$ reaction has been measured recently in the energy range $E_{c.m.} = 265 - 740$ keV[7, 8, 9]. It is dominated by the contribution of a new $3/2^+$ (s-wave) resonance at $E_x = 7.064$ MeV in ^{19}Ne and, at lower temperatures, by the $3/2^-$ state at 6.741 MeV[9]. The maximum angle-integrated cross section for the higher of the two resonances is ~ 250 mb, while for the proton capture reaction $^{18}\text{F}(\text{p},\gamma)^{19}\text{Ne}$ only an upper limit of 42 μb has been determined[10] so far.

With these cross sections the astrophysical reaction rates and, thus, the mean lifetimes of ^{18}F in a star can be calculated. The results for a star with a density $\rho = 5000$ g/cm³ and a mass fraction $X_H = 0.77$ are shown in Fig. 1 plotted as function of the temperature T_9 , where T_9 is the temperature in 10^9 K. Also included are the mean lifetimes for the $^{19}\text{Ne}(\text{p},\gamma)^{20}\text{Na}$ and $^{15}\text{O}(\alpha,\gamma)^{19}\text{Ne}$ reactions[11] using a mass fraction $X_{He} = 0.2$.

As can be seen, the lifetime of ^{18}F in hydrogen in this temperature region is dominated by the (p,α) reaction which destroys ^{18}F within less than 10^{-5} sec. The lifetime for converting ^{18}F via the (p,γ) reaction is typically 3 orders of magnitude larger and

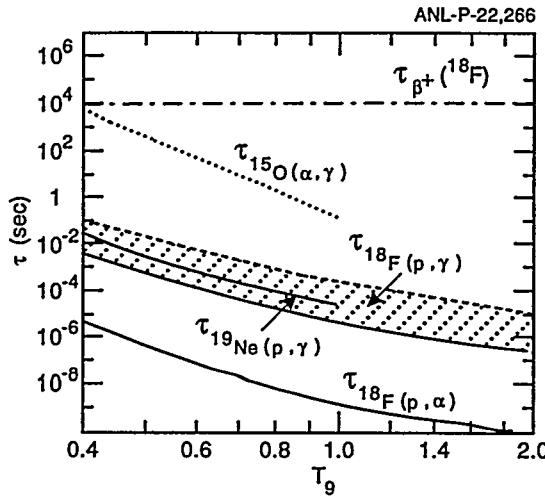


Figure 1. Mean lifetimes of ^{18}F , ^{19}Ne and ^{15}O in a star with a density $\rho=5000$ g/cm 2 as function of the temperature T_9 .

comparable with the lifetime of the $^{19}\text{Ne}(p,\gamma)^{20}\text{Na}$ reaction. Although the lifetime for producing ^{19}Ne via the $^{15}\text{O}(\alpha,\gamma)$ reaction is still 4-5 orders of magnitude higher, the amount of ^{15}O available in the stellar environment makes the $^{15}\text{O}(\alpha,\gamma)$ reaction the main route for generating ^{19}Ne . This was shown in a simplified network calculation involving the $^{18}\text{F}(p,\alpha)$, $^{18}\text{F}(p,\gamma)$ and $^{15}\text{O}(\alpha,\gamma)$ reactions. From the time dependence of the relative contributions for ^{18}F , ^{15}O and ^{19}Ne , respectively, it can be seen that due to the large $^{18}\text{F}(p,\alpha)$ reaction rate the ^{18}F material is immediately converted into ^{15}O , indicating that the $^{18}\text{F}(p,\gamma)^{19}\text{Ne}$ route is only a small branch for the production of ^{19}Ne , which is more efficiently produced via the $^{15}\text{O}(\alpha,\gamma)$ reaction.

4. The ^{56}Ni waiting point

The doubly closed shell nucleus ^{56}Ni is of considerable interest to astrophysics. ^{56}Ni is produced via helium burning in the core of massive stars, in supernova explosions and in the rp process[2]. The small Q-value ($Q=0.695$ MeV) for the (p,γ) proton capture reaction on ^{56}Ni makes this nucleus a 'waiting point' for the reaction flow towards heavier nuclei. For a realistic determination of the astrophysical reaction rate, detailed information on the structure (excitation energy and spectroscopic factors) of nuclei around $A=56$ is required.

We have therefore measured spectroscopic factors for low-lying states in ^{57}Ni , populated via the inverse $d(^{56}\text{Ni},p)^{57}\text{Ni}$ reaction using the 250 MeV ^{56}Ni beam described above. The beam bombarded a 500 $\mu\text{g}/\text{cm}^2$ CD_2 target located in the scattering chamber of the Fragment Mass Analyzer (FMA)[12]. Protons emitted at backward angles from the $d(^{56}\text{Ni},p)^{57}\text{Ni}$ reaction were detected in a large Si detector array consisting of a position-sensitive annular detector and six 5×5 cm 2 Si strip detectors (strip width 1 mm), covering a total solid angle of 2.8 sr. To separate the (d,p) reactions on ^{56}Ni from those induced by the ^{56}Co and ^{56}Fe beam impurities, the reaction products were identified by their mass and nuclear charge at the focal plane of the FMA in coincidence

with protons. For the Z identification of the reaction products it was necessary to use a passive absorber[13] consisting of a stack of ten Au foils with a total thickness of 7 mg/cm² that slowed down the Fe, Co and Ni particles differently.

A Q-value spectrum for protons from the d(⁵⁶Ni,p) reaction, as measured with the annular Si detector covering the angular range $\theta = 147^\circ - 162^\circ$ in coincidence with ⁵⁷Ni ions detected in the FMA is shown in Fig. 2a. In the center-of-mass system this range corresponds to forward angles for a (d,p) reaction, where transitions to low-spin

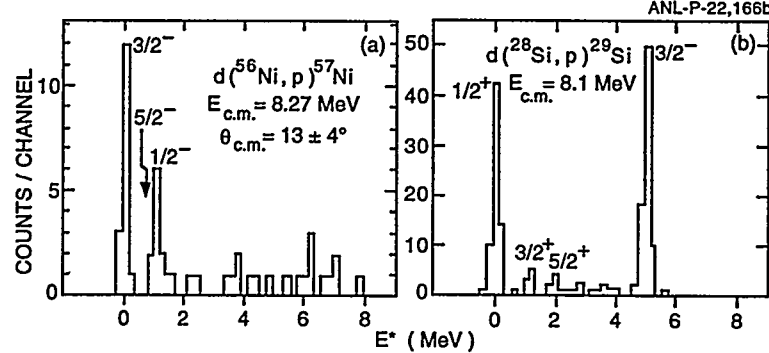


Figure 2. (a) Q-value spectrum measured at forward c.m. angles for the d(⁵⁶Ni,p)⁵⁷Ni reaction at $E(^{56}\text{Ni})=250$ MeV. (b) Q-value spectrum for the d(²⁸Si,p)²⁹Si reaction. In this angle range, only $l=0,1$ states are strongly populated

states ($l=0,1$) should be strongly populated. Indeed, the spectrum is dominated by the transitions to the $3/2^-$ ($E_x=0$ MeV) and the $1/2^-$ ($E_x=1.113$ MeV) states in ⁵⁷Ni while the yields for states at $E_x=2.5$ and $E_x=3.8$ MeV are considerably smaller indicating little single-particle strength for low-spin states in ⁵⁷Ni at higher excitation energy. The spectrum is quite different from the one obtained for the d(²⁸Si,p)²⁹Si reaction, where a strong population of the high-lying $2p_{3/2}$ single-particle state at $E_x=4.9$ MeV is observed (see Fig. 2b).

The angular distributions for the first three states in ⁵⁷Ni are presented in Fig. 3. The uncertainties in the measured differential cross sections include the statistical errors as well as uncertainties associated with beam current determination and detection efficiency. The solid lines in Fig. 3 are the result of DWBA calculations for the reaction mechanism with spectroscopic factors from shell-model calculations. The code PTOLEMY[14] was used with optical model parameters taken from the literature. A shell-model calculation was performed within a space containing the $f_{7/2}$, $f_{5/2}$, $p_{3/2}$ and $p_{1/2}$ orbitals with a Hamiltonian described in Ref.[15]. The configurations included 0, 1 and 2 particles excited out of the $f_{7/2}$ orbital. This calculations yielded spectroscopic factors of $S=0.91$ ($2p_{3/2}$), $S=0.91(1f_{5/2})$ and $S=0.90(2p_{1/2})$, respectively. With these spectroscopic factors good agreement between the experimental and the calculated angular distributions is obtained, indicating that these states in ⁵⁷Ni are indeed well characterized as the $2p_{3/2}$, $2p_{1/2}$ and $1f_{5/2}$ single-particle states. These angular distributions together with the low yields observed in the excitation energy region between 2-4 MeV, where higher lying $1/2^-$, $3/2^-$, and $5/2^-$ states are expected, support the fact that the

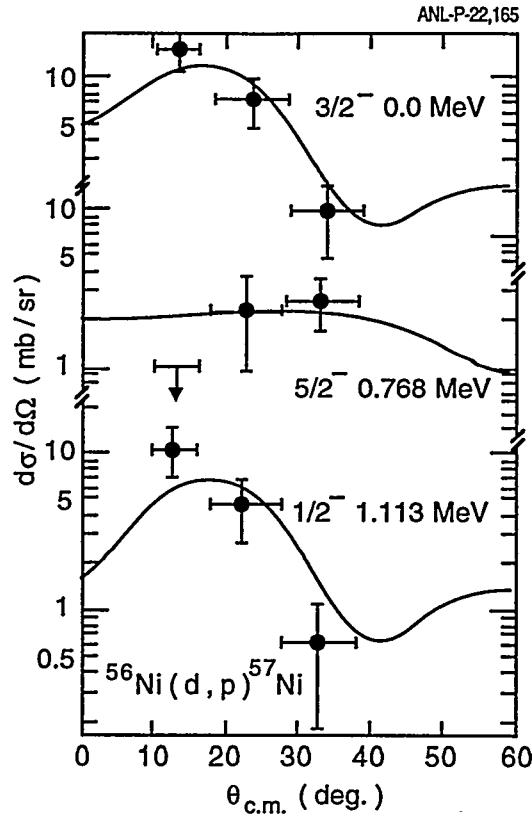


Figure 3. Differential cross sections as function of the center-of-mass angle θ_{cm} for the three lowest states populated in the $d(^{56}\text{Ni}, p)^{57}\text{Ni}$ reaction. The solid lines are the result of DWBA calculations.

main single particle strength for these low-spin states is concentrated in the first three excited states.

The observation of the single-particle structure of ^{57}Ni allows us to make predictions for the strength of the $^{56}\text{Ni}(p, \gamma)$ reaction leading to the mirror nucleus ^{57}Cu , which is crucial for the production of heavier proton-rich nuclei in explosive nucleosynthesis[16]. Because of the small Q-value, the yield of the radiative capture reaction depends on the excitation energies and the spectroscopic strengths of specific low-lying states in ^{57}Cu . The excitation energies of these states were determined recently[17]. At the temperatures occurring in typical nova and supernova explosions and in X-ray bursts ($T_9 \sim 0.5 - 1$), the main contribution comes from the low-lying ($E_x \leq 3$ MeV) $5/2^-$ and $1/2^-$ states. Assuming charge symmetry and using the same spectroscopic factors C^2S as measured for the mirror nucleus ^{57}Ni , we estimate the proton widths Γ_p for proton-unbound mirror states in ^{57}Cu from the expression:

$$\Gamma_p(E, \ell) = C^2 S \cdot \Gamma_p^{s.p.}(E, \ell) \quad (1)$$

The single particle widths $\Gamma_p^{s.p.}(E, \ell)$ were calculated in a Woods-Saxon potential with a radius parameter of $r_o = 1.25$ fm and a diffuseness of $a = 0.65$ fm or from R-matrix theory using a radius of 5.36 fm (see Ref.[6] for details).

The calculated astrophysical reaction rates are shown in Fig. 4 as a function of the temperature T_9 . In the critical temperature region $T_9 < 1$ the $1/2^-$ state completely dominates. Higher-lying states in ^{57}Cu with $E_x > 2.5$ MeV contribute only at temperatures $T_9 > 1$.

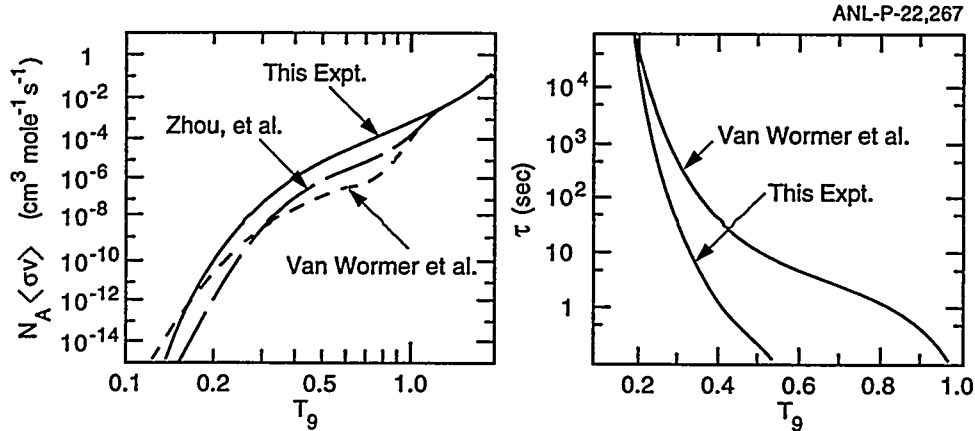


Figure 4. (a) Astrophysical reaction rates $N_A < \sigma v >$ for the $^{56}\text{Ni}(p,\gamma)^{57}\text{Cu}$ reaction. Also shown are the results from Refs. 3 and 17, respectively. (b) Lifetimes of ^{56}Ni calculated using the results from the present experiment and Ref. 3, respectively.

The dashed lines in Fig. 4a represents the result for the astrophysical reaction rate obtained in Refs. [17] and [3], respectively. Since these authors used a smaller proton width for the $1/2^-$ state [17] or a higher (p,γ) threshold [3] their estimates of the reaction rate for the $^{56}\text{Ni}(p,\gamma)^{57}\text{Cu}$ reaction are lower by more than an order of magnitude at temperatures below $T_9 = 1$.

The mean life of ^{56}Ni with respect to the (p,γ) reaction as function of the temperature T_9 is shown in Fig. 4b in comparison with the results of Ref.[3] As can be seen, a considerable decrease in the lifetime of ^{56}Ni is observed in the critical temperature region between $T_9=0.3 - 1$. This shorter lifetime will result in an increased production rate of elements and isotopes on the proton-rich side of the mass valley above ^{56}Ni .

The experiments described in this contribution were a collaborative effort between researchers at Argonne National Laboratory, Hebrew University, Jerusalem; University of Notre Dame, South Bend, IN; Northwestern University, Evanston, IL and University of Wisconsin, Madison, WI. This work was supported by U.S. Department of Energy, Nuclear Physics Division under contract No. W-31-109-ENG-38, the National Science Foundation and by a University of Chicago/Argonne National Laboratory Collaborative Grant.

References

[1] *Proc of the Fourth Int Conf on Radioactive Nuclear Beams, Omiya, Japan 1997* Nucl. Phys. A616 1

- [2] Champagne A E and Wiescher M 1992 *Annu. Rev. Nucl. Part. Sci* **42** 39
- [3] van Wormer L et al 1994 *Astrophys. J.* **432** 326
- [4] Mueller A C and Sherill B M 1993, *Annu. Rev. Nucl. Part. Sci* **43** 529
- [5] Roberts A et al 1995 *Nucl. Instrum. Methods Phys. Res.* **B103** 523
- [6] Rehm K E et al 1998 *Phys. Rev. Lett.* **80** 676
- [7] Rehm K E et al 1995 *Phys. Rev.* **C52** R460
- [8] Coszach R et al 1995 *Phys. Lett.* **B353** 184
- [9] Graulich J S et al 1997 *Nucl. Phys.* **A626** 751
- [10] Rehm K E et al 1997 *Phys. Rev.* **C55** R566
- [11] Smith M S 1990 *PhD thesis* Yale University (unpublished)
- [12] Davids C N et al 1992 *Nucl. Instrum. Methods Phys. Res.* **B70** 358
- [13] Henning W et al 1981 *Nucl. Instrum. Methods* **184** 247
- [14] MacFarlane M H and Pieper S C 1978 *Argonne National Laboratory Report* No. ANL-76-11(Rev.1)
- [15] Kraus G et al 1994 *Phys. Rev. Lett.* **73** 1773
- [16] Wiescher M et al 1998 *Phil. Trans. R. Soc. London A* (in print)
- [17] Zhou X G et al 1996 *Phys. Rev.* **C53**, 982